# Accepted Manuscript

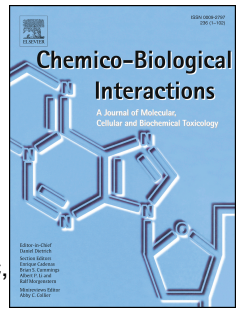


Mechanisms of redox interactions of bilirubin with copper and the effects of penicillamine

Bojana Božić, Jelena Korać, Dalibor M. Stanković, Marina Stanić, Ana Popović-Bijelić, Jelena Bogdanović Pristov, Ivan Spasojević, Milica Bajčetić

PII: S0009-2797(17)30782-2

DOI: 10.1016/j.cbi.2017.10.022

Reference: CBI 8127

To appear in: *Chemico-Biological Interactions*

Received Date: 18 July 2017

Revised Date: 10 October 2017

Accepted Date: 22 October 2017

Please cite this article as: B. Božić, J. Korać, D.M. Stanković, M. Stanić, A. Popović-Bijelić, J. Bogdanović Pristov, I. Spasojević, M. Bajčetić, Mechanisms of redox interactions of bilirubin with copper and the effects of penicillamine, *Chemico-Biological Interactions* (2017), doi: 10.1016/j.cbi.2017.10.022.

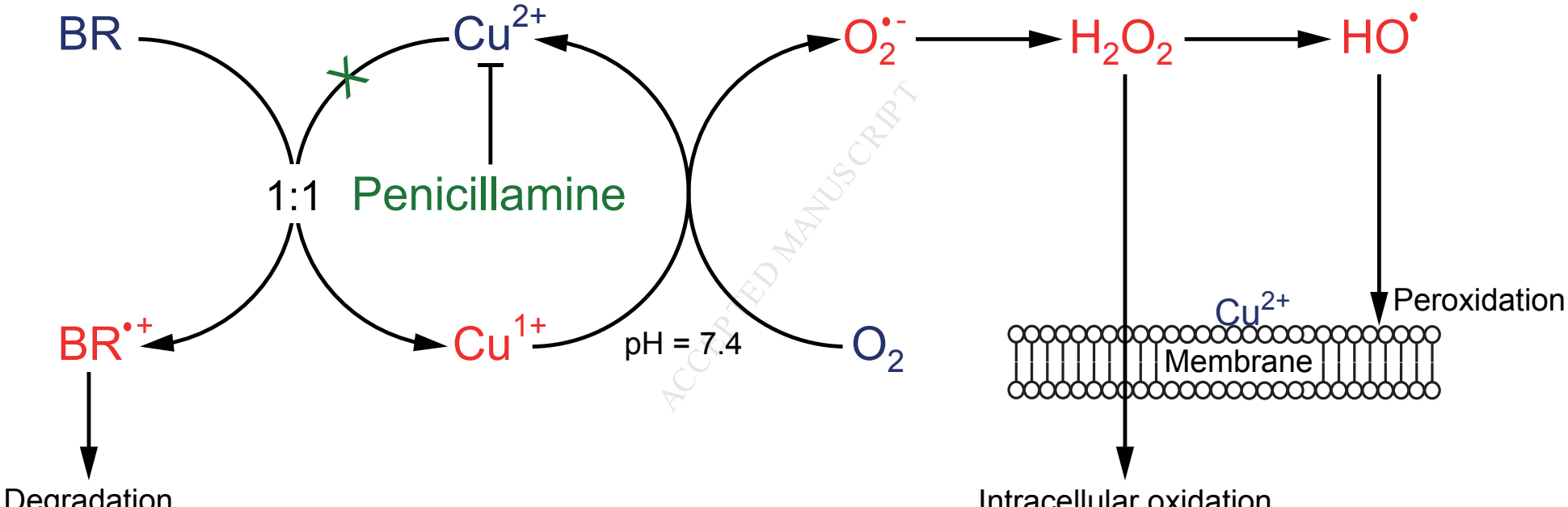

**Mechanisms of redox interactions of bilirubin with copper and the effects of penicillamine**

Bojana Božić,[a] Jelena Korać,[b] Dalibor M. Stanković,[c,d] Marina Stanić,[b] Ana Popović-Bijelić,[e] Jelena Bogdanović Pristov,[b] Ivan Spasojević,[b*] Milica Bajčetić[a,f]

[a]*Department of Pharmacology, Clinical Pharmacology and Toxicology, School of Medicine, University of Belgrade, P.O. Box 38, 11000 Belgrade, Serbia*

[b]*Life Sciences Department, Institute for Multidisciplinary Research, University of Belgrade, Kneza Višeslava 1, 11000 Belgrade, Serbia*

[c]*The Vinča Institute of Nuclear Sciences, University of Belgrade, POB 522, 11001 Belgrade, Serbia*

[d]*Department of Analytical Chemistry, Innovation Center of the Faculty of Chemistry, University of Belgrade, Studentski trg 12-16, Belgrade, 11000, Serbia*

[e]*EPR Laboratory, Faculty of Physical Chemistry, University of Belgrade, Studentski trg 12-16, 11158 Belgrade, Serbia*

[f]*Clinical Pharmacology Unit, University Children's Hospital, 11000 Belgrade, Serbia*

***Corresponding author**: Ivan Spasojević; Institute for Multidisciplinary Research, University of Belgrade, Kneza Višeslava 1, 11000 Belgrade, Serbia

Tel: +381 11 2078459; E-mail: redoxsci@gmail.com



Abbreviations: BR, bilirubin; DMPC, 1,2-Dimyristoyl-sn-glycero-3-phosphorylcholine; EPR, electron paramagnetic resonance; MDA, malondialdehyde; PA, penicillamine.

**Abstract**

Toxic effects of unconjugated bilirubin (BR) in neonatal hyperbilirubinemia have been related to redox and/or coordinate interactions with $Cu^{2+}$. However, the development and mechanisms of such interactions at physiological pH have not been resolved. This study shows that BR reduces $Cu^{2+}$ to $Cu^{1+}$ in 1:1 stoichiometry. Apparently, BR undergoes degradation, *i.e.* BR and $Cu^{2+}$ do not form stable complexes. The binding of $Cu^{2+}$ to inorganic phosphates, liposomal phosphate groups, or to chelating drug penicillamine, impedes redox interactions with BR. $Cu^{1+}$ undergoes spontaneous oxidation by $O_2$ resulting in hydrogen peroxide accumulation and hydroxyl radical production. In relation to this, copper and BR induced synergistic oxidative/damaging effects on erythrocytes membrane, which were alleviated by penicillamine. The production of reactive oxygen species by BR and copper represents a plausible cause of BR toxic effects and cell damage in hyperbilirubinemia. Further examination of therapeutic potentials of copper chelators in the treatment of severe neonatal hyperbilirubinemia is needed.

**Keywords:** Erythrocytes; Hydrogen peroxide; Hyperbilirubinemia; Lipid peroxidation; Superoxide

## 1. Introduction

Hyperbilirubinemia, the accumulation of bilirubin (BR) in the plasma and tissues, is often observed in newborns. It develops due to high turnover of erythrocytes and hepatic immaturity, but also in relation to some pathological conditions, such as hemolytic diseases and sepsis [1,2]. BR levels exceeding physiological concentrations more than 20-fold, labeled as severe hyperbilirubinemia, may result in neural damage, promoted hemolysis and general cellular injury, and increased risk of sepsis [3–5]. The treatment of severe hyperbilirubinemia relies on exchange transfusions, which show considerable rate of complications (~10%), including infections, venous thrombosis, thrombocytopenia, and necrotizing enterocolitis [3,6]. In order to develop safer therapeutic approaches, it is essential to understand the molecular mechanisms of BR toxicity.

It has been recognized that pathologic phenotypes of hyperbilirubinemia are primarily due to unconjugated BR (not bound to albumin) [7]. BR is produced in the second step of heme (porphyrin) catabolic pathway via two-electron reduction of biliverdin [8]. As such, BR represents an electron-rich molecule with potential to form multiple coordinate bonds (*e.g.* via N in four pyrrole moieties), with specific redox-active metals [9]. Pertinent to this, it has been contemplated that detrimental effects of hyperbilirubinemia may come from redox/coordinate interactions of BR with copper [10]. There is a substantial amount of indirect evidence for this: (i) several clinical studies have found beneficial effects of copper-chelation therapy with penicillamine (PA) in neonatal hyperbilirubinemia [11–13]; (ii) neonates with hyperbilirubinemia show increased plasma levels of copper [14]; (iii) neural injury in hyperbilirubinemia occurs primarily in basal ganglia [3], which show higher copper content compared to other brain regions [15]; and (iv) a number of studies have found signs of oxidative stress, including lipid peroxidation and depletion of major antioxidants - ascorbate and thiols, in the plasma of neonates with hyperbilirubinemia [16–18]. On the other hand, reports on BR-$Cu^{2+}$ biochemistry at physiological pH are inconsistent, proposing the formation of stable coordination complexes with different stoichiometries [19–21], as well as $Cu^{2+}$ reduction by BR with accompanying generation of reactive oxygen species [22,23]. It is worth mentioning that some studies of BR-$Cu^{2+}$ system have been performed at pH > 8 [24,25]. Those appear to be of little relevance for explaining processes in the plasma (pH = 7.4), taking into account that pK values for BR are above 8 [26].

We set out to examine in detail the interactions of BR and $Cu^{2+}$ at plasma pH, and to evaluate the effects of PA on this system, using spectrophotometry, electrochemical methods, and electron paramagnetic resonance (EPR) spectroscopy. In addition, biochemical assays were applied to examine the effects of BR and copper on the membrane of human erythrocytes.

## 2. Material and Methods

### 2.1. Chemicals

All chemicals were of analytical grade: BR (>98% purity), $CuCl_2$, D-penicillamine, catalase (CAT; C1345), 1,2-dimyristoyl-*sn*-glycero-3-phosphocholine (DMPC), buffer components (Sigma-Aldrich, St. Louis, MO, USA), CuCl (Merck, Kenilworth, NJ, USA), $FeCl_3$ (Analytika Ltd., Prague, Czech Republic). All experiments were performed using bidistilled deionized ultrapure (18 MΩ) water. Stock solutions of BR (1 mM) in 5 mM NaOH, PA, and CuCl (prepared in 1 M HCl; an aliquot of 1 M NaOH was used to neutralize the acid), as well as phosphate buffer (50 mM $KH_2PO_4$; pH 7.4), and phosphate buffer saline (PBS: 10 mM $Na_2HPO_4$, 2 mM $KH_2PO_4$, 137 mM NaCl, 2.7 mM KCl; pH 7.4) were prepared each day, and kept light-protected on ice if needed. Incubation and measurements were conducted in the dark at 293 K, except for experiments with erythrocytes (310 K).

### 2.2. UV/VIS spectroscopy

UV-Vis absorption spectra were obtained using 2501 PC Shimadzu spectrophotometer (Kyoto, Japan), using the following settings: sample volume, 1 mL; scan range 800–250 nm; scan time, 50 s; initial scan, 30 s after sample preparation; follow up period, 30 min.

### 2.3. Cyclic and differential pulse voltammetry

The voltammetric measurements were performed using a potentiostat/galvanostat CHI 760b (CH Instruments Inc., Austin, TX, USA), controlled by corresponding electrochemical software. The electrochemical cell was equipped with a boron-doped diamond electrode embedded in a polyether ether ketone body with an inner diameter of 3 mm, resistivity of 0.075 Ω cm, and boron doping level of 1000 ppm (Windsor Scientific Ltd., Slough, UK). This was the working electrode, with Ag/AgCl (3 M KCl) reference electrode (potentials reported in this paper are referred versus this electrode), and a Pt wire as a counter electrode. Scan rate was 0.1 V/s. Differential pulse voltammetry was performed on the same instrument using the following settings: initial *E*, 0.5 V; final *E*, -0.5 V; increment, 0.004 V; amplitude, 0.05 V; pulse width, 0.05 s; sample width, 0.01 s; quiet time, 2 s. Cyclic voltammetry measurements were performed in water, pH 5. The pH of each system was measured after mixing all components, and carefully adjusted to ~5 with HCl (100 mM). The established aliquots of HCl were added to BR solution or water prior to the formation of each system. Measurements were initiated immediately after sample preparation.

### 2.4. EPR spectroscopy

Measurements at 110 K were conducted on a Bruker Elexsys-II EPR spectrometer operating at X-band (9.4 GHz), with Bruker $N_2$ Temperature Controller ER4131VT, and the following settings: microwave power, 3.17 mW; scan time, 80 s; modulation amplitude, 0.5 mT; modulation frequency, 100 kHz;

number of accumulations, 4. All spectra were baseline corrected. DMPC liposomes (62.5 mg/mL final concentration of lipids) were prepared in water according to the previously described protocol [27]. Samples were placed in quartz EPR tubes and quickly frozen in cold isopentane after 30 s of incubation.

2.5. Oximetry

The concentration of $O_2$ was determined using a Clark type oxygen electrode (Hansatech Instruments Ltd., King's Lynn, UK) operating with Lab Pro interface and Logger Pro 3 software (Vernier, Beaverton, OR, USA). All systems were recorded for 2–5 min before the addition of BR to establish the stability of baseline and zero rate of $O_2$ change. Decrease in [$O_2$] was monitored for 10 min and then CAT (200 IU) was added to determine the concentration of $H_2O_2$, which corresponds to the double concentration of CAT-induced $O_2$ release (mechanism of CAT activity: $2H_2O_2 \rightarrow 2H_2O + O_2$) [28].

2.6. Effects on erythrocytes

Erythrocytes were obtained from five healthy volunteers using Vacutainer tubes containing $K_3$EDTA as the anticoagulant (BD, Franklin Lakes, NJ, USA), and centrifugation (2000 g/10 min/4$^{o}$C). Buffy coat was carefully removed, and erythrocytes were washed 3× and re-suspended in PBS. Following 5 min of incubation at 310 K with gentle shaking, supernatants were collected by centrifuged. Malondialdehyde (MDA) levels were measured using previously described method [29]. In brief, MDA reacts with thiobarbituric acid in acidic conditions at 100$^{o}$C to form pink colored complex. MDA concentration was calculated using the absorbance at 535 nm and molar extinction coefficient of $1.56 \times 10^5$ L mol$^{-1}$ cm$^{-1}$. Extracellular Hb was measured as cyanmethemoglobin using the Drabkin method [30].

2.7. Statistical analysis

All experiments were performed at least in triplicate (experiments on erythrocytes were repeated five times). Data are presented as mean ± S.D. Statistical significance was established via nonparametric two-tailed Mann–Whitney U test (for two sample groups) or one-way ANOVA with *post hoc* Duncan's range test (for >2 sample groups). The limit of statistical significance was $p < 0.05$.

**3. Results and Discussion**

UV-Vis spectrophotometry was applied to investigate potential development of BR:$Cu^{2+}$ complexes (the formation of coordinate bonds results into the *d*-orbital splitting that may lead to absorption in the visible range), or BR degradation. It can be observed that the characteristic band of BR ($\lambda_{max}$ = 435 nm) was diminished within 10 min in the presence of copper, and that the maximum was shifted to 400 nm (Fig. 1a). In parallel with this, a weak line at 330 nm and a broad 'tail' in the upper field,

emerged. The intensity of $\lambda_{max}$ = 400 nm peak and the 'tail' further decreased with time, whereas an additional line at $\lambda_{max}$ ~655 nm slowly developed. The later may come from a small amount of biliverdin (about 20 μM; calculated from UV-Vis spectra of biliverdin (not shown)), which has $\lambda_{max}$ at 670 nm [31]. Changes in the UV-Vis spectra imply that BR and $Cu^{2+}$ do not form stable complex(es). The results speak in favor of $Cu^{2+}$-induced degradation of BR with multiple derivatives and secondary products. This is in accordance with previous reports on the irreversible degradation of BR that was exposed to oxidizing agents [31]. In the absence of copper, BR was stable in the phosphate buffer (Fig. 1b). Only a small decrease in the intensity of 435 nm band was observed, which may be attributed to precipitation, since BR is not deprotonated/charged at pH = 7.4 [26]. Similar results were obtained in the presence of $Fe^{3+}$, implying that BR and $Fe^{3+}$ do not develop coordinate or redox interactions. This can be put into the context of Pearson HSAB principle. Pyrrole is a borderline Lewis base, whereas $Cu^{2+}$ and $Fe^{3+}$ are a borderline acid and a hard acid, respectively [32]. Accordingly, the affinity of BR is higher for $Cu^{2+}$ than for $Fe^{3+}$. $Cu^{2+}$ and BR probably form a transient complex, which is followed by electron transfer.

Cyclic voltammetry was applied to examine redox behavior of copper in the presence of BR. The experiments were conducted in water (pH ~5), because copper-related currents were attenuated in the phosphate buffer. Pertinent to this, speciation diagrams implicate complete solubility of $Cu^{2+}$ in water at pH 5, which was not the case for phosphate buffer at pH 7.4 (Supplementary Fig. 1). $Cu^{2+}$ and $Cu^{1+}$ showed peak currents ($i_p$) at different oxidation/anodic ($E_{pa}$) and reduction/cathodic ($E_{pc}$) potentials (Fig. 2a). The assignation was in accordance with the standard potentials of $Cu^{2+}$ and $Cu^{1+}$ [33]. All these peaks were present in cyclic voltammograms of the system with $Cu^{2+}$ and BR, but with weaker $i_p$ (Fig. 2b), probably because of the adhesion/interference of BR on/with the electrode surface. Still, changes of $i_p$ of $Cu^{2+}$ (at $E_{pa}$ = 265 mV and $E_{pc}$ = -217 mV) and $Cu^{1+}$ (at $E_{pa}$ = 135 mV and $E_{pa}$ = 534 mV) were evident. Currents assigned to $Cu^{1+}$ showed a time-dependent drop that was accompanied by the rise of $Cu^{2+}$ currents. Apparently, BR induced a reduction of $Cu^{2+}$ to $Cu^{1+}$, which was followed by spontaneous oxidation of $Cu^{1+}$. To determine the stoichiometry of BR-induced reduction of $Cu^{2+}$, a differential pulse voltammetry of $i_{pc}$ of $Cu^{2+} \rightarrow Cu^{1+}$ was applied (Fig. 2c). Using a calibration curve, it was determined that the concentration of remaining $Cu^{2+}$ in the system with initial $Cu^{2+}$ and BR concentrations of 0.4 and 0.2 mM, respectively, was 0.25 ± 0.04 mM. In other words, the amount of $Cu^{2+}$ that was reduced was similar to BR concentration, implying that BR reduces $Cu^{2+}$ in 1:1 stoichiometry. This is in accordance with some previous estimates [21].

Low-T EPR is a method of choice for examining $Cu^{2+}$ complexes [34]. It also delivers info on $Cu^{2+}$ reduction, since $Cu^{1+}$ is an EPR 'silent' species ($S$ = 0). Voltammetry showed that BR-induced reduction of $Cu^{2+}$ was fast (Fig. 2), so the EPR spectra were collected after 30 s incubation period. Fig.

3a shows characteristic EPR spectrum of $Cu^{2+}$ in axial symmetry with one strong $g_{\perp}$ line and four weak lines coming from hyperfine coupling with $^{63}Cu/^{65}Cu$ nuclei ($I$ = 3/2) along $g_{\parallel}$ [35]. The signal was drastically decreased in the presence of BR. This is in line with the proposed BR-induced reduction of $Cu^{2+}$ to $Cu^{1+}$, and with the absence of stable BR:$Cu^{2+}$ complex(es) at physiological pH. Although the concentration ratio between BR and $Cu^{2+}$ was 1:1, not all $Cu^{2+}$ was reduced, which appears not to be in accord with the results obtained by differential pulse voltammetry (Fig. 2c). However, the discrepancy could be easily explained by different speciation of $Cu^{2+}$ in phosphate buffer at pH 7.4 (EPR experiments), compared to copper in water at pH 5 (voltammetry). Namely, a fraction of $Cu^{2+}$ at pH 7.4 is present in the form of a non-soluble phosphates (Supplementary Fig. 1), which may not be accessible for BR-induced reduction. The remaining $Cu^{2+}$ signal in the presence of BR showed a broader $g_{\perp}$ line compared to the initial $Cu^{2+}$ spectrum, whereas lines from hyperfine coupling could not be observed. This may be a result of inhomogenous broadening due to anisotropic interactions or an unresolved hyperfine structure of $Cu^{2+}$ in the solid state [36].

Next, we examined whether chelating agent PA can prevent BR-induced reduction. The spectrum of $Cu^{2+}$ in the presence of PA appears to include two components: a broad signal of $Cu^{2+}$ chelated by PA, and the signal of $Cu^{2+}$ in the phosphate buffer (Fig. 3b). The broadening of the signal of PA-bound $Cu^{2+}$ has been attributed to the dipolar interactions between multiple paramagnetic $Cu^{2+}$ ions within PA-copper clusters [37]. The incubation with BR diminished the signal of 'free' $Cu^{2+}$, whereas the signal of $Cu^{2+}$-PA complex was only slightly affected. This implies that $Cu^{2+}$ within the cluster is inaccessible to BR. In addition, we were interested whether BR can reduce $Cu^{2+}$ that is bound to phospholipids [38]. DMPC liposomes were used as a model membrane. The spectrum of $Cu^{2+}$ in the presence of liposomes showed $g$-values that were similar to the position of lines for $Cu^{2+}$ in the phosphate buffer (Fig. 3c). This implies that $Cu^{2+}$ binds to phospholipids via phosphate groups, which show very low pKa values and hence bear negative charges [39]. BR did not significantly affect the intensity of signal of liposome-bound $Cu^{2+}$, but it caused some broadening of $g_{\perp}$ line. This implicates that $Cu^{2+}$ bound to membranes is poorly accessible to BR. The broadening might be related to formation of BR-phospholipid aggregates [40], which could affect the organization of liposomes and their interactions with $Cu^{2+}$.

Oximetry was applied to further examine the stoichiometry and the involvement of $O_2$ in redox interactions between BR and $Cu^{2+}$. It is known that $Cu^{1+}$ rapidly reacts with molecular oxygen at physiological pH to produce superoxide radical anion, which is further reduced/dismutated to $H_2O_2$ [41,42]. The addition of BR to $Cu^{2+}$ solutions induced a drastic drop in the concentration of $O_2$ (Fig. 4a). The decrease of [$O_2$] was only slightly pronounced in systems with [$Cu^{2+}$]/[BR] > 1 concentration ratio compared to the system with [$Cu^{2+}$]/[BR] = 1 (142 ± 4 µM *vs.* 129 ± 11 µM; $p > 0.05$). In addition,

the amount of consumed $O_2$ in the system with $[Cu^{2+}]/[BR] = 0.5$ was approximately one half of $O_2$ consumed in $[Cu^{2+}]/[BR] = 1$ system. This further substantiates that one BR 'generates' one $Cu^{1+}$. The consumption of $O_2$ in $[Cu^{2+}]/[BR] = 1$ system was significantly suppressed by PA (80 ± 15 μM; p = 0.040). Following 10 min incubation period, CAT was added to estimate the concentration of $H_2O_2$. The incubation of 0.2 mM $Cu^{2+}$ with 0.2 mM BR led to the accumulation of a significant amount of $H_2O_2$ (69 ± 17 μM). In the presence of 0.2 mM PA in this system, the concentration of accumulated $H_2O_2$ was halved (33 ± 11 μM; p = 0.044) (Fig. 4b). It is important to note that although PA has the capacity to bind both $Cu^{2+}$ and $Cu^{1+}$, it shows much higher affinity for the latter [43]. The level of $O_2$ in all examined systems was not completely reversed by the addition of CAT. Clearly, some amount of $H_2O_2$ is lost, most likely via Fenton-like reaction that generates highly reactive hydroxyl radical ($Cu^{1+} + H_2O_2 \rightarrow Cu^{2+} + OH^- + HO^\bullet$) [44].

Redox interactions of BR and copper result in the formation of $Cu^{1+}$ and the production of $H_2O_2$ and $HO^\bullet$. $Cu^{1+}$ and $HO^\bullet$ may initiate lipid peroxidation and damage cell membranes [45], whereas $H_2O_2$ crosses the membrane to 'hit' intracellular targets [28]. Pertinent to this, the effects of BR-$Cu^{2+}$ system on human erythrocytes and the protective capacity of PA were examined, using extracellular MDA and hemoglobin as markers of lipid peroxidation and hemolysis (Fig. 5). It is important to note that $Cu^{2+}$ was applied at concentration that matches the range previously reported for the plasma of neonates with hyperbilirubinemia [14]. It can be observed that $Cu^{2+}$ and BR induced lipid peroxidation and hemolysis, which is in line with previous reports [46,47]. Such effects have been related to redox interactions of $Cu^{2+}$ with cellular membranes [45,47], and to the mechanical effects of BR on erythrocyte membrane [48]. Importantly, lipid peroxidation and hemolysis were significantly more pronounced in erythrocytes exposed simultaneously to $Cu^{2+}$ and BR. PA alleviated the damage, but the markers of peroxidation and hemolysis were still higher compared to control values. It is plausible that PA prevents pro-oxidative activity of $Cu^{2+}$ in the presence of BR via sequestration, whereas the direct effects of BR on the membranes remained. It is important to note here that the plasma concentrations of unconjugated BR in severe hyperbilirubinemia have been estimated at ~20 nM [7]. So the direct effects of BR on cell membranes might be less important compared to the synergistic effects of $Cu^{2+}$ and BR.

In conclusion, BR reduces $Cu^{2+}$ (to $Cu^{1+}$) in 1:1 stoichiometry. This is accompanied by $Cu^{1+}$-induced reduction of $O_2$ that results in $H_2O_2$ accumulation and $HO^\bullet$ production. The sequestration of copper by PA diminished redox interplay and alleviated the damaging effects on membranes. The binding of $Cu^{2+}$ to liposomes prevented BR-induced reduction, but it appears that such mechanism does not take place at erythrocytes membrane. The elucidated mechanisms warrant further research on the potential benefits of copper-chelation therapy in the treatment of neonatal hyperbilirubinemia. It is

noteworthy that PA appears not to exhibit significant short-term side-effects in infants [49]. In addition, other copper-sequestrating agents are available (triethylenetetramine; appears to show less side-effects in adults compared to PA), or are being tested for the treatment of Wilson's disease (*e.g.* tetrathiomolybdate) [50].

**Competing financial interests**

The authors declare no competing financial interests.

**Acknowledgments**

The work was supported by the Ministry of Education, Science and Technological Development of the Republic of Serbia, Grant No. OI173014 and OI173017. D.M.S wishes to acknowledge Magbiovin project (FP7-ERA Chairs-Pilot Call-2013, Grant Agreement: 621375). The EPR spectra were acquired in the EPR Laboratory, Faculty of Physical Chemistry, University of Belgrade.

**Appendix A. Supplementary data**

Supplementary data related to this article can be found at:

**References**


[1] B.O. Olusanya, F.B. Osibanjo, T.M. Slusher, Risk factors for severe neonatal hyperbilirubinemia in low and middle-income countries: a systematic review and meta-analysis, Plos One. 10 (2015) e01172229.

[2] R.J. Wong, D.K. Stevenson, Neonatal hemolysis and risk of bilirubin-induced neurologic dysfunction, Semin. Fetal Neonatal Med. 20 (2015) 26–30.

[3] P.A. Dennery, D.S. Seidman, D.K. Stevenson, Neonatal hyperbilirubinemia, N. Engl. J. Med. 344 (2001) 581–590.

[4] M. Kaplan, R. Bromiker, C. Hammerman, Hyperbilirubinemia, hemolysis, and increased bilirubin neurotoxicity, Semin. Perinatol. 38 (2014) 429–437.

[5] F. Raimondi, A.C. Borrelli, T. Ferrara, A. Giannattasio, L. Capasso, Bilirubin exposure is associated with neonatal sepsis in the eight days preceding symptoms: a retrospective study, J. Matern. Fetal Neonatal Med. 30 (2017) 2078–2080.

[6] American Academy of Pediatrics Subcommittee on Hyperbilirubinemia, Management of hyperbilirubinemia in the newborn infant 35 or more weeks of gestation, Pediatrics. 114 (2004) 297–316.

[7] C.V. Hulzebos, P.H. Dijk, Bilirubin-albumin binding, bilirubin/albumin ratios, and free bilirubin levels: where do we stand? Semin. Perinatol. 38 (2014) 412–421

[8] A. Kikuchi, S.Y. Park, H. Miyatake, D. Sun, M. Sato, T. Yoshida, Y. Shiro, Crystal structure of rat biliverdin reductase, Nat. Struct. Biol. 8 (2001) 221–225.

[9] J.D. Van Norman, M.M. Humans, Bilirubin–metal ion complexes. Anal. Chem. 46 (1974) 926–929.

[10] C. Mancuso, Bilirubin and brain: A pharmacological approach, Neuropharmacology 118 (2017) 113–123.

[11] L. Lakatos, B. Kövér, G. Oroszlán, Z. Vekerdy, D-penicillamine therapy in ABO hemolytic disease of the newborn infant, Eur. J. Pediatr. 123 (1976) 133–137.

[12] L. Lakatos, B. Kövér, S. Vekerdy, E. Dvorácsek, D-penicillamine therapy of neonatal jaundice: comparison with phototherapy, Acta Paediatr. Acad. Sci. Hung. 17 (1976) 93–102.

[13] L. Lakatos, G. Balla, I. Pataki, Z. Vekerdy-Nagy, G. Oroszlán, D-Penicillamine in the neonatal period: Case reports, Int. J. Med. Pharm. Case Rep. 4 (2015) 59–63.

[14] K.H. Schulpis, T. Karakonstantakis, S. Gavrili, C. Costalos, E. Roma, I. Papassotiriou, Serum copper is decreased in premature newborns and increased in newborns with hemolytic jaundice, Clin. Chem. 50 (2004) 1253–1256.

[15]P. Ramos, A. Santos, N.R. Pinto, R. Mendes, T. Magalhães, A. Almeida, Anatomical region differences and age-related changes in copper, zinc, and manganese levels in the human brain, Biol. Trace Elem. Res. 161 (2014) 190–201.

[16]K.K. Abdul-Razzak, M.K. Nusier, A.D. Obediat, A.M. Salim, Antioxidant vitamins and hyperbilirubinemia in neonates, Ger. Med. Sci. 5 (2007) Doc03.

[17]Y. Altuner Torun, U. Ertural, A.B. Ergul, C. Karakukcu, A.M. Akin, Reduction in serum paraoxonase level in newborns with hyperbilirubinemia as a marker of oxidative stress, J. Matern. Fetal. Neonatal Med. 30 (2016) 2297–2300.

[18]S. Basu, D. De, H. Dev Khanna, A. Kumar, Lipid peroxidation, DNA damage and total antioxidant status in neonatal hyperbilirubinemia, J. Perinatol. 34 (2014) 519–523.

[19]J.R. Ferraro, J. Wu, R.D. Soloway, W. Li, Y. Xu, D. Xu, G. Shen, Copper binding to bilirubin as determined by FT-IR and EPR spectroscopy, Appl. Spectrosc. 50 (1996) 922–927.

[20]S. Adhikari, R. Joshi, C. Gopinathan, Bilirubin as an anti precipitant against copper mediated denaturation of bovine serum albumin: formation of copper-bilirubin complex, Biochim. Biophys. Acta. 1380 (1998) 109–114.

[21]S.F. Asad , S. Singh, A. Ahmad, N.U. Khan, S.M. Hadi, Prooxidant and antioxidant activities of bilirubin and its metabolic precursor biliverdin: a structure-activity study, Chem. Biol. Interact. 137 (2001) 59–74.

[22]S.F. Asad, S. Singh, A. Ahmad, S.M. Hadi, Bilirubin-Cu(II) complex degrades DNA, Biochim. Biophys. Acta. 1428 (1999) 201–208.

[23]S.F. Asad SF, S. SingH, A. Ahmad, S.M. Hadi, Bilirubin/biliverdin-Cu(II) induced DNA breakage; reaction mechanism and biological significance, Toxicol. Lett. 131 (2002) 181–189.

[24]J. He, X.D. Lu, X. Zhou, N. Yu, Z. Chen, Surface-enhanced Raman spectroscopy of bilirubin-metal ion complexes, Biospectroscopy 1 (1995) 157–162.

[25]I Sóvágó , B. Harman, I. Kolozsvári, F. Matyuska, Complex-formation and redox reactions of bilirubin and biliverdin with zinc(II), . cadmium( II) and copper( II) ions, Inorg. Chim. Acta 106 (1985) 181–186.

[26]J.D. Ostrow, P. Mukerjee, Revalidation and rationale for high pKa values of unconjugated bilirubin, BMC Biochem. 8 (2007) 7.

[27]M. Rangel, A. Leite, A.M.N. Silva, T. Moniz, A. Nunes, M.J. Amorim, C. Queirós, L. Cunha-Silva, P. Gameiro, J. Burgess, Distinctive EPR signals provide an understanding of the affinity of bis-(3-hydroxy-4-pyridinonato) copper(II) complexes for hydrophobic environments, Dalton Trans. 43 (2014) 9722–9731.

[28]M. Mojić, J. Bogdanović Pristov, D. Maksimović-Ivanić , D.R. Jones, M. Stanić, S. Mijatović, I. Spasojević , Extracellular iron diminishes anticancer effects of vitamin C: an in vitro study. Sci. Rep. 4 (2014) 5955.

[29]H. Ohkawa, N. Ohishi, K. Yagi, Assay for lipid peroxidesin animal tissues by thiobarbituric acid reaction, Anal. Biochem. 95 (1979) 351–358.

[30]D.L. Drabkin, J.H. Austin, Spectrophotometric studies. II. Preparations from washed blood cells; nitric oxide hemoglobin and sulfhemoglobin, J. Biol. Chem. 112 (1935) 51–65.

[31]A.F. McDonagh, The biliverdin-bilirubin antioxidant cycle of cellular protection: Missing a wheel? Free Radic. Biol. Med. 49 (2010) 814–820.

[32]K.L. Haas, K.J. Franz, Application of metal coordination chemistry to explore and manipulate cell biology, Chem. Rev. 109 (2009) 4921–4960.

[33]W.M. Haynes, CRC Handbook of Chemistry and Physics, 95th ed., CRC Press Taylor & Francis Group, Boca Raton, 2014.

[34]A.C. Rosenzweig, Bioinorganic chemistry: Zeroing in on a new copper site, Nat. Chem. 1 (2009) 684–685.

[35]W.R. Hagen, EPR spectroscopy as a probe of metal centres in biological systems. Dalton Trans. 37 (2006) 4415–4434.

[36]J.A. Weil, J.R. Bolton, Electron Paramagnetic Resonance. Elementary Theory and Practical Applications, second ed., John Wiley & Sons Inc., Hoboken, 2007.

[37]P.J. Birker, H.C. Freeman, Structure, properties, and function of a copper(I)-copper(II) complex of D-penicillamine: pentathallium(I) μ8-chloro-dodeca (D-penicillaminato)-octacuprate(I)hexacuprate(II) *n*-hydrate, J. Am. Chem. Soc. 99 (1977) 6890–6998.

[38]M.F. Poyton, A.M. Sendecki, X. Cong, P.S. Cremer, Cu(2+) Binds to phosphatidylethanolamine and increases oxidation in lipid membranes, J. Am. Chem. Soc. 138 (2016) 1584–1590.

[39]D. Marsh, Handbook of Lipid Bilayers, CRC Press, Boca Raton, 2013.

[40]E.F. Eriksen, H. Danielsen, R. Brodersen, Bilirubin-liposome interaction. Binding of bilirubin dianion, protonization, and aggregation of bilirubin acid, J. Biol. Chem. 256 (1981) 4269–4274.

[41]D.K. Johnson, M.J. Stevenson, Z.A. Almadidy, S.E. Jenkins, D.E. Wilcox, N.E. Grossoehme, Stabilization of Cu(I) for binding and calorimetric measurements in aqueous solution. Dalton Trans. 44 (2015) 16494–16505.

[42]K. Reybier, S. Ayala, B. Alies, J.V. Rodrigues, S. Bustos Rodriguez, G. La Penna, F. Collin, C.M. Gomes, C. Hureau, P. Faller, Free superoxide is an intermediate in the production of $H_2O_2$ by copper(I)-Aβ peptide and $O_2$, Angew. Chem. Int. Ed. Engl. 55 (2016) 1085–1089.

[43]N. Kato, M. Nakamura, T. Uchiyama, 1H NMR studies of the reactions of copper(I) and copper(II) with D-penicillamine and glutathione, J. Inorg. Biochem. 75 (1999) 117–121.

[44]I. Spasojević, M. Mojović, Z. Stević, S.D. Spasić, D.R. Jones, A. Morina, M.B. Spasić, Bioavailability and catalytic properties of copper and iron for Fenton chemistry in human cerebrospinal fluid, Redox Rep. 15 (2010) 29–35.

[45]E.T. Horsley, M.J. Burkitt, C.M. Jones, R.A. Patterson, L.K. Harris, N.J. Moss, J.D. del Rio, D.S. Leake, Mechanism of the antioxidant to pro-oxidant switch in the behavior of dehydroascorbate during LDL oxidation by copper(II) ions, Arch. Biochem. Biophys. 465 (2007) 303–314.

[46]D. Brites, R. Silva, A. Brito, Effect of bilirubin on erythrocyte shape and haemolysis, . under hypotonic, aggregating or non-aggregating conditions, and correlation with cell age. Scand. J. Clin. Lab. Invest. 57 (1997) 337–349.

[47]A. Fernandes, M.L. Mira, M.S. Azevedo, C. Manso, Mechanisms of hemolysis induced by copper, Free Radic. Res. Commun. 4 (1988) 291–298.

[48]M.A. Brito, C.D. Brondino, J.J. Moura, D. Brites, Effects of bilirubin molecular species on membrane dynamic properties of human erythrocyte membranes: a spin label electron paramagnetic resonance spectroscopy study, Arch. Biochem. Biophys. 387 (2001) 57–65.

[49]M.J. Qureshi, M. Kumar, D-Penicillamine for preventing retinopathy of prematurity in preterm infants, Cochrane Database Syst. Rev. 2013 (2013) CD001073.

[50]P. Delangle, E. Mintz, Chelation therapy in Wilson's disease: from D-penicillamine to the design of selective bioinspired intracellular Cu(I) chelators, Dalton Trans. 41 (2012) 6359–6370.

FIGURE LEGENDS

**Fig. 1.** UV-Vis spectra of bilirubin (BR) in the absence or presence of $Cu^{2+}$ or $Fe^{3+}$ in 50 mM phosphate buffer, pH 7.4. (**a**) Changes in spectra of 0.1 mM BR in the presence of 0.2 mM $Cu^{2+}$ during 30 min (spectra were acquired every 5 min). Changes are marked with arrows. (**b**) Spectra of 0.1 mM BR before and after 30 min of incubation in the absence or the presence of 0.2 mM $Fe^{3+}$.
Color: in online only.

**Fig. 2.** Cyclic and differential pulse voltammograms of copper and bilirubin (BR)-$Cu^{2+}$ in water, pH ~5, at boron-doped diamond electrode. (**a**) Cyclic voltammograms (scan rate 0.1 V/s) of 0.1 mM CuCl and 0.4 mM $CuCl_2$ with labeled peak current oxidation/anodic ($E_{pa}$) and reduction/cathodic ($E_{pc}$) potentials. (**b**) Changes (marked with arrows in the enlargement) in cyclic voltammograms (scan rate 0.1 V/s) of copper in the presence of 0.2 mM BR. Arrowhead marks a time-depended decrease of the current at $E_{pa}$ = -217 mV. (**c**) Differential pulse voltammograms (increment, 0.004 V; pulse width, 0.05 s; sample width, 0.01 s; quiet time, 2 s) of $Cu^{2+}$ at different concentrations in the absence or the presence of 0.2 mM BR.
Color: in online only.

**Fig. 3.** 110 K EPR spectra of $Cu^{2+}$ in the absence or the presence of 0.2 mM bilirubin (BR) after 30 s incubation period. (**a**) 0.2 mM $Cu^{2+}$, and 0.2 mM $Cu^{2+}$ + BR, in 50 mM phosphate buffer, pH 7.4. Arrowheads – positions of 4 lines coming from the hyperfine splitting along $g_{\parallel}$. $\Delta B_{\perp}$ – line widths of $g_{\perp}$ signals before and after the incubation with BR. (**b**) 0.2 mM $Cu^{2+}$ + 0.2 mM penicillamine (PA) in the absence or the presence of BR in 50 mM phosphate buffer, pH 7.4. Arrow – a broad line of penicillamine-bound $Cu^{2+}$. (**c**) $Cu^{2+}$ + liposomes, and $Cu^{2+}$ + liposomes + BR in water. Dotted line: 0.2 mM $Cu^{2+}$ in the phosphate buffer (for reference).

**Fig. 4.** The consumption of molecular oxygen in different bilirubin (BR)-$Cu^{2+}$ systems in 50 mM phosphate buffer, pH 7.4. (**a**) Changes in $O_2$ concentration and $O_2$ consumption rate induced by the addition of BR to $Cu^{2+}$ solutions. (**b**) The effects of 0.2 mM PA on $O_2$ consumption (rate) in the system with 0.2 mM $Cu^{2+}$ and 0.2 mM BR. $H_2O_2$ accumulation was quantified 10 min after the addition of BR, by CAT-induced $O_2$ release ($2H_2O_2 \rightarrow 2H_2O + O_2$). Arrowheads – artifact that emerged with BR supplementation. Color: in online only.

**Fig. 5.** Effects of 10 μM bilirubin (BR) and 10 μM $Cu^{2+}$ on erythrocytes, in the absence or the presence of 20 μM penicillamine (PA) following 5 min incubation at 37$^{o}$C in the phosphate buffer saline, pH 7.4. (**a**) The extracellular concentration of the product of lipid peroxidation – MDA. (**b**) The amount of extracellular hemoglobin, which is a marker of hemolysis. Bars not sharing a common letter are significantly different ($p < 0.05$; one-way ANOVA with *post hoc* Duncan's range test).

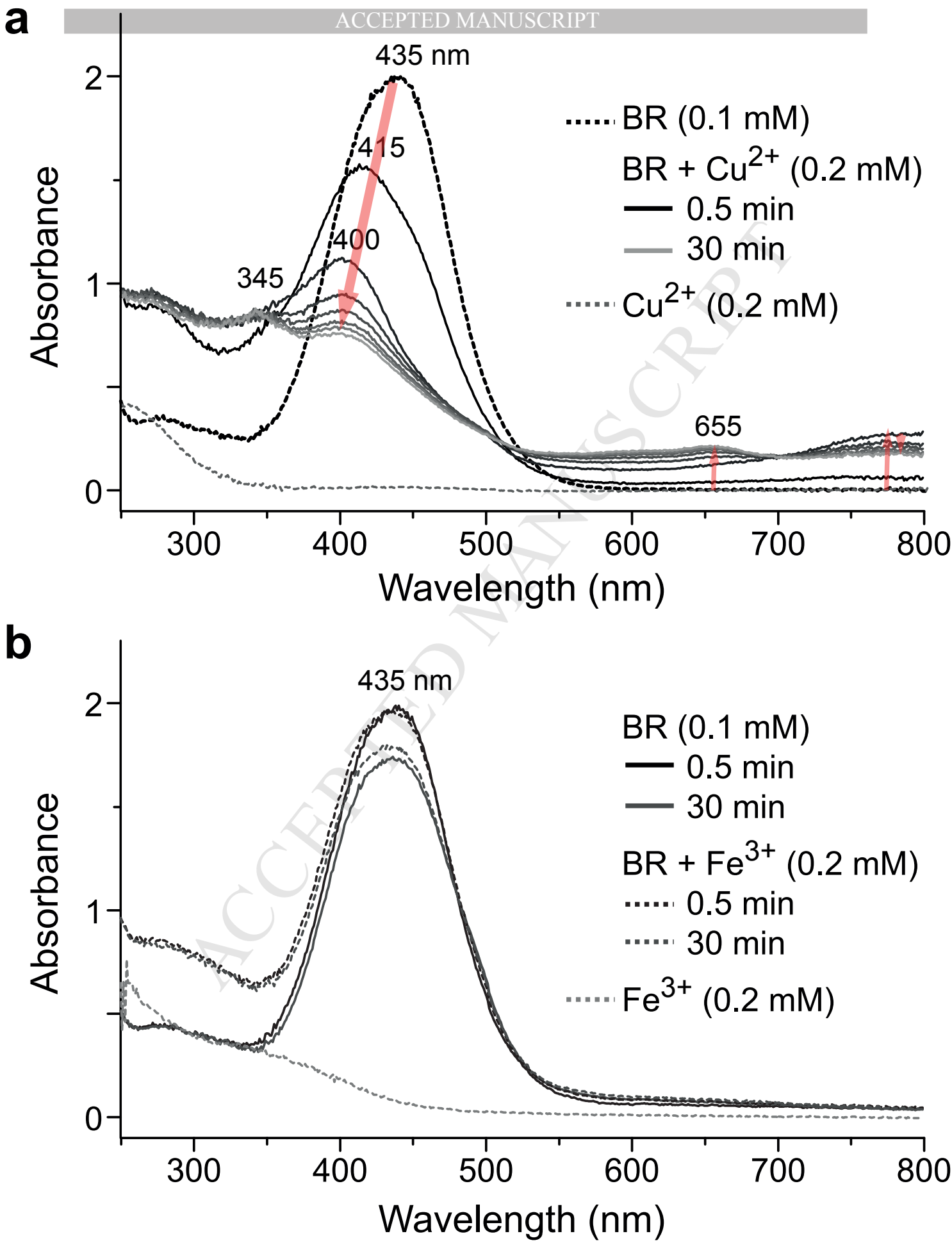

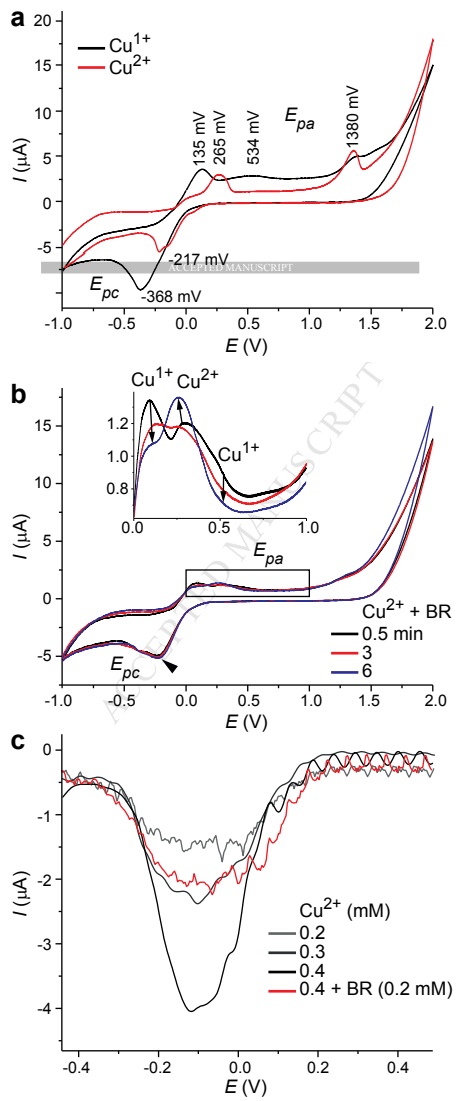

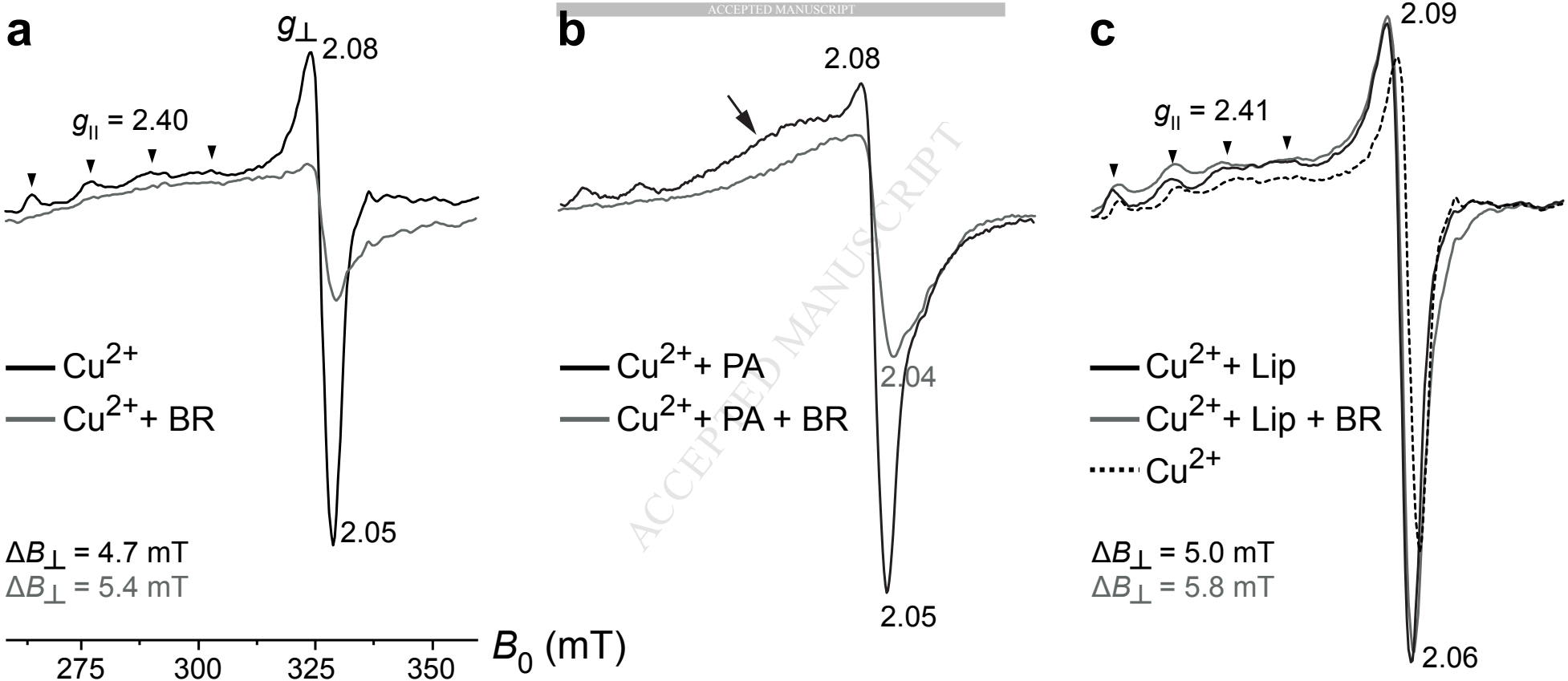

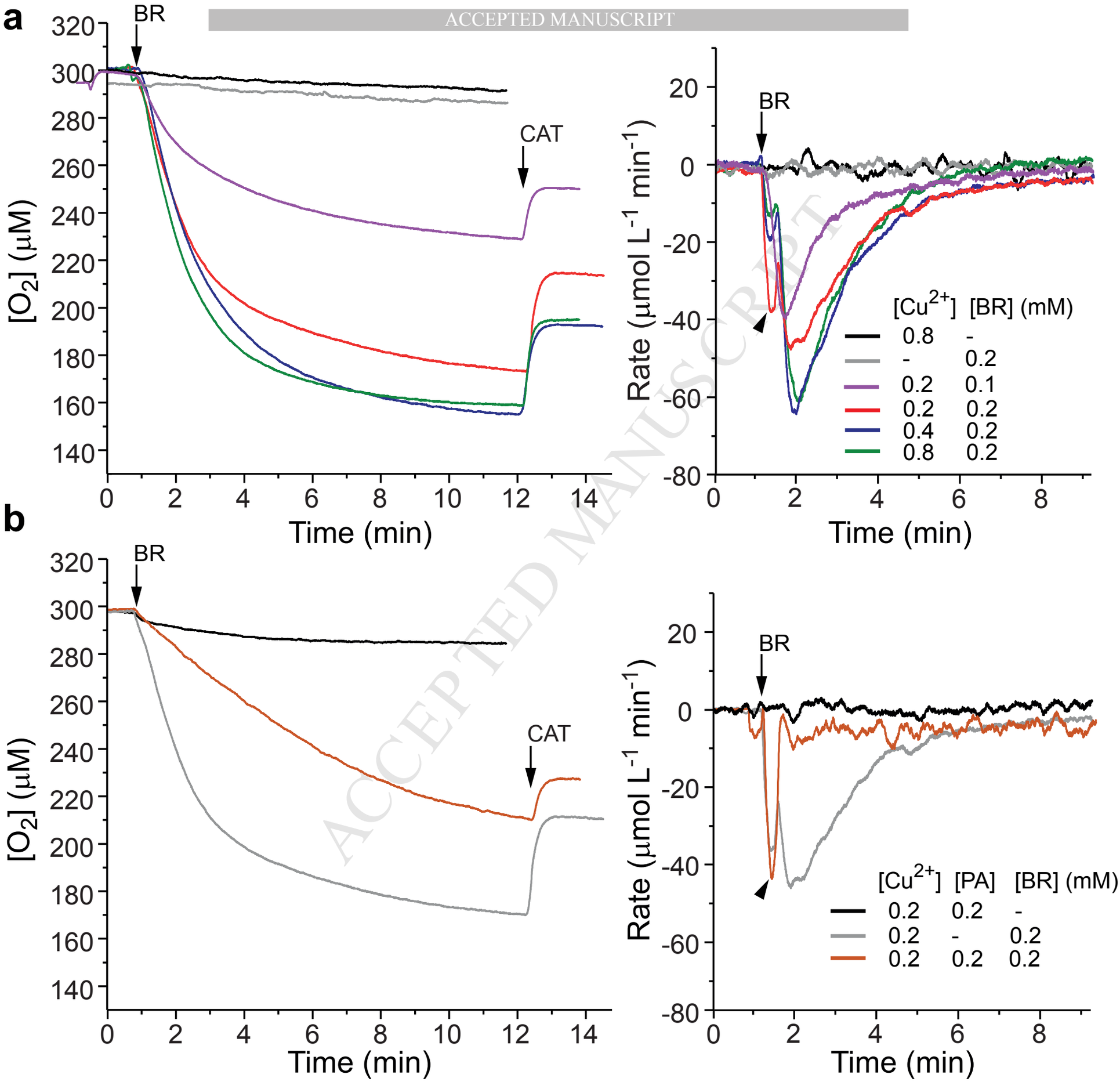

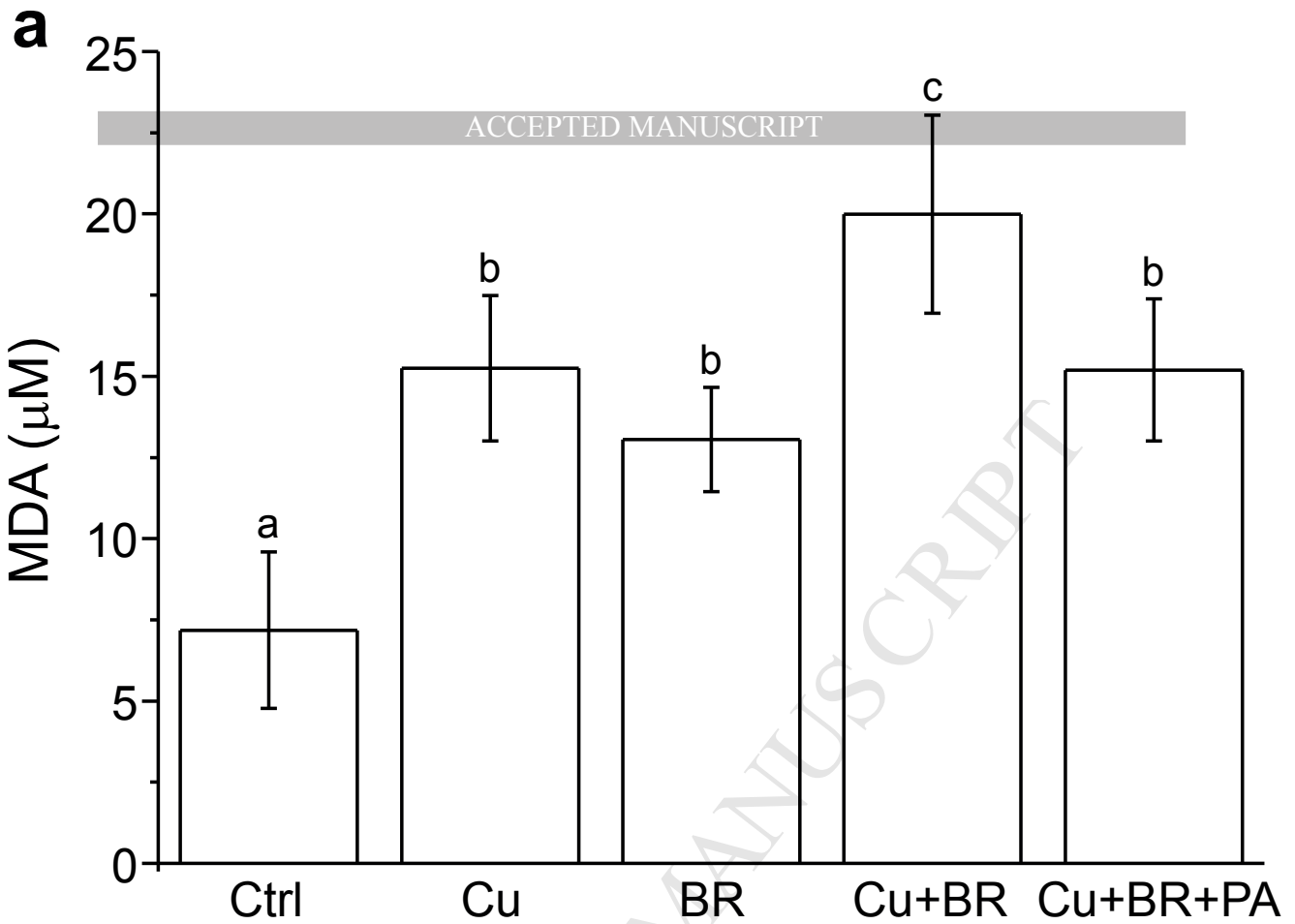


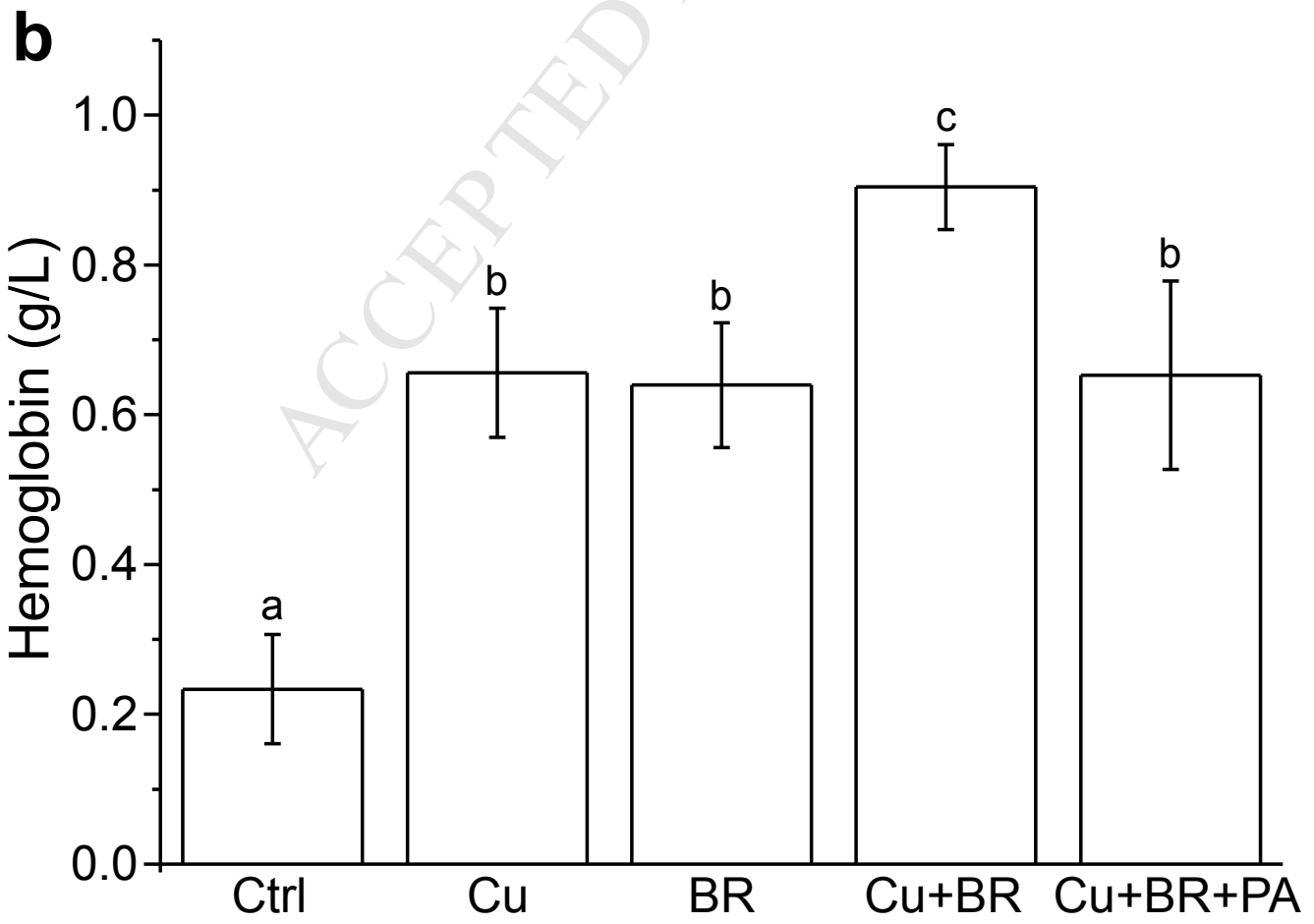

– Bilirubin reduces $Cu^{2+}$ in 1:1 stoichiometry

– $Cu^{1+}$ undergoes spontaneous oxidation resulting in reactive oxygen species production

– Copper and bilirubin induce oxidative damage in cell membranes

– Redox interactions of $Cu^{2+}$ and bilirubin are hampered by penicillamine and phosphates